Journal of Orthopaedic Translation (2019) 18, 128–141

Available online at www.sciencedirect.com

ScienceDirect

journal homepage: http://ees.elsevier.com/jot

ORIGINAL ARTICLE

Optimization of electrospray fabrication of stem cell–embedded alginate–gelatin microspheres and their assembly in 3D-printed poly(ε-caprolactone) scaffold for cartilage tissue engineering

Yichi Xu [a,b], Jiang Peng [a], Geoff Richards [b], Shibi Lu [a,**], David Eglin [b,*]

[a] Lab of Orthopaedics of Department of Orthopaedics, Chinese PLA General Hospital, Beijing Key Lab of Regenerative Medicine in Orthopaedics, Key Lab of Musculoskeletal Trauma & War Injuries of PLA, Beijing 100853, China
[b] AO Research Institute Davos, Clavadelerstrasse 8, 7270 Davos Platz, Switzerland

Received 6 March 2019; received in revised form 10 May 2019; accepted 26 May 2019
Available online 25 June 2019

KEYWORDS
3D printing;
Alginate–gelatin;
biofabrication;
Cartilage tissue engineering;
Electrospray

Abstract *Objective:* Our study reports the optimization of electrospray human bone marrow stromal cell (hBMSCs)–embedded alginate–gelatin (Alg-Gel, same as following) microspheres for the purpose of their assembly in 3D-printed poly(ε-caprolactone) (PCL) scaffold for the fabrication of a mechanically stable and biological supportive tissue engineering cartilage construct.
Methods: The fabrication of the Alg-Gel microspheres using an electrospray technique was optimized in terms of polydispersity, yield of microspheres and circularity and varying fabrication conditions. PCL scaffolds were designed and printed by melt extrusion. Then, four groups were set: Alg-hBMSC microspheres cultured in the 2D well plate (Alg-hBMSCs+2D) group, Alg-Gel-hBMSC microspheres cultured in the 2D well plate (Alg-Gel-hBMSCs+2D) group, Alg-Gel-hBMSC microspheres embedded in PCL scaffold cultured in the 2D well plate (Alg-Gel-hBMSCs+2D) group and Alg-Gel-hBMSCs microspheres cultured in the 3D bioreactor (Alg-Gel-hBMSCs+3D) group. Cell viability, proliferation and chondrogenic differentiation were evaluated, and mechanical test was performed.
Results: Nonaggregated, low polydispersity and almost spherical microspheres of average diameter of 200–300 μm were produced with alginate 1.5 w: v%, gelatin (Type B)

* Corresponding author. AO Research Institute Davos, Clavadelerstrasse 8, 7270 Davos Platz, Switzerland.
** Corresponding author. Lab of Orthopaedics of Department of Orthopaedics, Chinese PLA General Hospital, Beijing Key Lab of Regenerative Medicine in Orthopaedics, Key Lab of Musculoskeletal Trauma & War Injuries of PLA, Beijing 100853, PR China.
E-mail addresses: lushibi301@163.com (S. Lu), david.eglin@aofoundation.org (D. Eglin).

https://doi.org/10.1016/j.jot.2019.05.003

concentration of 0.5 w: v % and $CaCl_2$ coagulating bath concentration of 3.0 w: v %, using 30G needle size and 8 kV and 0.6 bar voltage and air pressure, respectively. Alginate with gelatin hydrogel improved viability and promoted hBMSC proliferation better than alginate microspheres. Interestingly, hBMSCs embedded in microspheres assembled in 3D-printed PCL scaffold and cultured in a 3D bioreactor were more proliferative in comparison to the previous two groups ($p < 0.05$). Similarly, the GAG content, GAG/DNA ratio as well as Coll 2 and Aggr gene expression were increased in the last two groups.

Conclusion: Optimization of hBMSC-embedded Alg-Gel microspheres produced by electrospray has been performed. The Alg-Gel composition selected allows conservation of hBMSC viability and supports proliferation and matrix deposition. The possibility to seed and assemble microspheres in designed 3D-printed PCL scaffolds for the fabrication of a mechanically stable and biological supportive tissue engineering cartilage construct was demonstrated.

Translational potential of this article: We optimize and demonstrate that electrospray microsphere fabrication is a cytocompatible and facile process to produce the hBMSC-embedded microsize tissue-like particles that can easily be assembled into a stable construct. This finding could have application in the development of mechanically competent stem cell —based tissue engineering of cartilage regeneration.

Introduction

Articular cartilage is a highly organized tissue with considerable resilience. However, it has limited intrinsic healing capacity upon alterations caused by trauma, ageing and diseases [1]. The management of articular cartilage defects is one of the most challenging clinical problems for orthopaedic surgeons [2]. Tissue engineering (TE) aims to develop biological substitutes that can restore the functions of altered tissues [1,3]. Cartilage TE has greatly benefited from recent advances in material engineering, stem cells and their interactions in tissue regeneration [4].

In this context, stem cells are generally seeded onto a scaffold or within a matrix, whose primary objective is to replicate some of the characteristics of the target-tissue extracellular matrix (ECM) and support chondrogenesis [5]. Hydrogels have attracted strong attention for applications in TE and regenerative medicine owing to their three-dimensional (3D) ECM-mimicking polymeric network, swelling ability and porous framework allowing for cell embedding [6,7]. Among the commonly used polymers for fabrication of hydrogels for cartilage TE, alginate (Alg) is widely studied. It is a polysaccharide with structural resemblance to the ECM glycosaminoglycans [8]. It is a natural polymer extracted from brown algae. Alginate gels are extensively studied for TE applications as a cell encapsulation material as well as an injectable 3D matrix for in vivo cell delivery [9]. Stem cell—embedded alginate microspheres can be produced and easily handled in vitro for stem cell chondrogenic differentiation and microtissue formation [10,11]. The major drawbacks of alginates are their low cell adhesiveness, poor support of cell proliferation and relative weak mechanical properties in comparison to cartilage tissue [12]. The lack of cell adhesiveness and proliferation can be addressed by simply adding gelatin to alginate [13]. Toughening of alginate gel can be achieved by chemical modification and formation of double network [14]. However, both biological and mechanical properties required for cartilage TE have not yet been optimized using such approach.

Interestingly, 3D-printed technologies such as fuse deposition modelling are more and more easy to use, allowing the fabrication of biomaterial constructs with controlled internal porosity and relevant mechanical properties in regard to cartilage repair.

Thus, the goal of this study was to demonstrate the possibility to combine electrosprayed human bone marrow stromal cell (hBMSC)—embedded alginate—gelatin (Alg-Gel) microspheres and a 3D-printed poly(ε-caprolactone) (PCL) scaffold for the fabrication of a mechanically stable and biologically supportive TE cartilage construct.

First, the fabrication of the Alg-Gel microspheres using an electrospray technique was optimized. The embedding of hBMSCs did not significantly influence the initial circularity, size and homogeneity of the produced microspheres. The selected Alg-Gel composition preserved hBMSC viability and supported in vitro chondrogenesis in comparison to alginate microspheres. Furthermore, seeding and assembly of microspheres in 3D-printed PCL scaffolds was achieved, and biochemical assays as well as gene expression analyses indicated that hBMSC chondrogenic potential was conserved. Lastly, the compressive modulus of the 3D-printed PCL scaffold with hBMSC-embedded Alg-Gel microspheres was assessed following 42 days of culture.

Material and methods

Isolation and culture of hBMSCs

Bone marrow was obtained from vertebral bodies of a single human donor (male, 48 years) under local anaesthesia after approval by the local ethical committee (ethic number: 325/08 Albert-Ludwigs-Universität Freiburg) and obtaining written

informed consent. hBMSCs were isolated and expanded according to a reported method [15]. hBMSCs were plated at a seeding density of 5×10^3 cells/cm^2 in Minimum Essential Medium Alpha (α-MEM) (Gibco, Paisley, UK) containing 10% foetal bovine serum (FBS) (Gibco), 100 U ml^{-1} of penicillin and 100 mg ml^{-1} of streptomycin. Cells were expanded in α-MEM containing 100 U ml^{-1} of penicillin/streptomycin, 10% FBS and 5 ng ml^{-1} basic fibroblast growth factor at 37 °C in 5% CO_2 atmosphere. The medium was changed every two days. hBMSCs from passage three to passage five were used in the three independent experiments.

Microsphere generating device—electrospray

Microsphere generation was performed using an electrospray device from Spraybase, Ireland. The electrospray device was composed of a high voltage supply (0—30 kV from the emitter to the collector) and an air pressure controller (with the maximum fluidic capacity 250 ml and pressure output 0.0—1.0 bar). The voltage and fluidic control were controlled using a ten-turn potentiometer dial located at the front panel. Voltage and air pressure were adjusted to 8/1.0, 6/1.0, 8/0.6 kV/bar, respectively. Two sizes of needle emitters of 27 and 30 G, supplied by Adhesive Dispensers Systems, UK, were used and placed at a constant height of 10 cm from the ground target collection vessel which was a 90-mm circular stainless-steel dish containing 30 ml of solutions of calcium chloride ($CaCl_2$, granulated, $\geq$97%, cat.n. 21074, Sigma, USA) in distilled water at 1 and 3% w/v concentration. Finally, a laser coupled with a camera connected to a computer was used to illuminate the plume/Taylor cone for visualization and optimization.

Preparation of microspheres

Sodium alginate (Alg) (powder, from brown algae, cat. n. 71238, Sigma, USA) was dissolved in distilled water at room temperature at a concentration of 1.5% w/v. Gelatin (Gel) (powder, from porcine skin, Type A, cat. n. 48722, Sigma, USA) was dissolved in distilled water at 40 °C with a concentration of 0.0, 1.0 and 2.5% w/w. Gelatin (powder, from bovine skin, Type B, cat. n. G9391, Sigma, USA) was dissolved in distilled water at 40 °C at a concentration of 0.5, 1.5 and 2.5% w/w. Alginate and gelatin solutions of different concentrations were mixed thoroughly at a 1:1 volume ratio to prepare an Alg-Gel solution; then, entrapped air bubbles were removed by centrifugation at 300 rpm/min for 3 min. Influence of the electrospray setting parameters such as voltage, air pressure and emitter diameter size was varied together with the Alg-Gel ratios and concentration of $CaCl_2$ solutions, and the manufactured microspheres were characterized for their morphology by optical microscopy. For the hBMSC-containing microspheres, hBMSCs were first evenly suspended in the Alg and Alg-Gel solutions at a concentration of 10^6 cells/ml and then manufactured into microspheres using optimized electrospray protocol. hBMSC-containing microspheres were collected soon after formation (10 min) in the collector bath ($CaCl_2$ in distilled water) and washed twice in 1 $\times$ phosphate-buffered saline.

Morphological characterizations of microspheres

After electrospray, the Alg-Gel microspheres and Alg-Gel-hBMSCs microspheres were collected and imaged by light microscopy using an AxioVert. A1, Carl Zeiss, Germany, in phase contrast. Fifty microspheres (n = 50) were randomly chosen for each group, and their diameters, circularity and polydispersity were measured using image analysis software (Image J Fiji 1.52b, USA).

hBMSC viability

hBMSC viability was determined by trypan blue staining. Briefly, 200 μl of cell-containing microspheres produced by electrospray or alginate drops produced using a 1-ml pipette (control) were dissolved in 800 μl of 55 mM sodium citrate solution before adding 0.1 ml of 0.4% w/v trypan blue solution. A haemocytometer was loaded to examine immediately the samples under a microscope at 10x magnification. The number of dead (blue-stained) cells and the number of total cells were counted. Three different fields were counted for each group and 3 technical replicates were performed. Cell viability was calculated as (number of total cells—number of dead cells)/number of total cells $\times$ 100%. The data were analysed and plotted using GraphPad Prism (version 7.00; GraphPad Software Inc., USA).

3D printing of poly(ε-caprolactone)

The design of macroporous cylindrical scaffold for loading with cell-laden microspheres was performed on BioCAD software (BioCAD 1.1, RegenHU Ltd. Switzerland). The diameter and the height of the scaffolds were 12 mm and 5 mm, respectively. For the initial printed layer, a line space of 200 μm between struts, lower than the average diameter of the microspheres, was printed to prevent microsphere leak out from the interspace. All the other layers had a line space of 800 μm. The layer-by-layer deposition was performed in a crisscross fashion forming an open columnar porosity from bottom to top. A 3D printer (3D Discovery, RegenHU Ltd.) equipped with a screw-based extruder was used for printing the PCL (Sigma—Aldrich, USA, Mn 45′000 g/mol) at a temperature of 75 °C and 70 °C for the printing head and polymer reservoir, respectively. The inner diameter of the printing head was 0.33 mm with a length of 11.2 mm, the screw rotation speed was set at 15 rpm and the printing speed was set up to 6 mm/s.

Cell culture experiments

In a first experiment, hBMSC proliferation was compared over a period of 14 days in the following groups: (i) 1.5% (w/w) Alg microspheres with 10×10^6 hBMSCs/ml cultured in a 2D well plate (Alg + 2D); (ii) 1.5% (w/w) Alg—0.5% (w/w) Gel microspheres with 10×10^6 hBMSCs/ml cultured in a 2D well plate (Alg-Gel + 2D); (iii) 1.5% (w/w) Alg—0.5% (w/w) Gel microspheres with 10×10^6 hBMSCs/ml laden in a 3D-printed PCL scaffold cultured in a 2D well plate (Alg-Gel + PCL + 2D) and (iv) 1.5% (w/w) Alg—0.5% (w/w) Gel

microspheres with 10×10^6 hBMSCs/ml cultured in a 3D bioreactor (Alg-Gel + 3D).

The growth medium contained α-MEM supplied with 100 U/ml of penicillin/streptomycin, 10% FBS and 5 ng/ml basic fibroblast growth factor. The medium was changed every two days. Static/2D culture of hBMSCs within microspheres (Alg + 2D, Alg-Gel + 2D and Alg-Gel + PCL + 2D) was performed in 12-well plates. For the 3D bioreactor group (Alg-Gel + 3D), 1×10^6 hBMSCs/ml within 1.5% (w/w) Alg—0.5% (w/w) Gel microspheres were cultured in a rotary cell culture system (RCCS; Synthecon, Houston). To facilitate the adhesion of microspheres, rotation was set as 20 rpm for 1 min with a 30-min pause for the first 24 h, and then, a continuous rotation at 50 rpm was kept constant for the following days. The RCCS was kept at 37 °C, 5% CO_2 in an incubator.

In a second experiment, the chondrogenic differentiation of hBMSCs within the 4 groups was assessed. A chondrogenic differentiation medium, containing DMEM (4.5 g/l glucose), ITS + (6.25 μg/ml insulin, 6.25 μg/ml transferrin and 6.25 μg/ml selenous acid (Gibco)), 100 mM dexamethasone, 0.17 mM L-ascorbic acid 2-phosphate, 1 mM sodium pyruvate, 0.35 mM L-prolin and 10 ng/ml TGF-β1 was used, and cells were cultured for up to 42 days. The culture medium was changed every two days.

Cell viability and proliferation

Cell viability and proliferation of hBMSCs cultured within the 4 groups were assessed by Live/Dead Cell Viability Assay (Sigma, St. Louis, USA) and CellTiter-Blue assay (Promega AG, Switzerland) after 2 h, and 3, 5, 7 and 14 days. Briefly, for Live/Dead staining, microspheres were rinsed with phosphate-buffered saline and immersed in 1 mL of serum-free medium containing 10 μM calcein AM stock and 1 μM ethidium homodimer in a 24-well plate. To ensure diffusion of dyes throughout, the sample were incubated with in the Live/Dead solution for 3 h at 4 °C followed by 1 h in an incubator set at 37 °C, 5% CO_2 and 90% humidity [16]. Images were collected with a confocal microscopy (LSM 800, Laser Scanning Confocal, Carl Zeiss Microscopy, Thornwood, USA). For the cell proliferation assay, 20 μl of CellTiter 96 AQueous One Solution Cell Proliferation (Promega, USA) reagent and 100 μl of medium were added into a well containing 20 μl of microsphere suspension and then kept for 2 h in an incubator set at 37 °C, 5% CO_2 and 90% humidity. 50 μl of supernatant was taken, and the absorbance was read at 490 nm using a plate reader (Victor, PerkinElmer). The data were normalized to those quantified at the 2-h time point. Empty microspheres were subjected to the same process as the cell-containing microspheres and used as blank. Nine technical replicates were performed for each group.

1,9-dimethylmethylene blue and Picogreen assays

Samples were digested with sodium citrate solution overnight. Subsequently, the total sulfated glycosaminoglycans content was determined by 1,9-dimethylmethylene blue dye assay (cat. n. 341088, Sigma, USA) using shark chondroitin sulphate as standard. The DNA content was quantified using a Quant-i PicoGreen dsDNA Assay Kit (Molecular Probes, Thermo Fisher Scientific, USA) according to the manufacturer's protocol. GAG/DNA ratio was calculated and plotted using GraphPad Prism (version 7.00; GraphPad Software Inc., USA)

RNA isolation and real-time polymerase chain reaction

For assessment of gene expression, constructs were placed in 1 ml TRI reagent supplemented with 5 μl polyacryl carrier (both from Molecular Research Center, Cincinnati, USA). Subsequently, samples were frozen at −20 °C until further analysis. After thawing, total cellular RNA was isolated using a modified TRIspin method [17]. Briefly, 1-bromo-3-chloropropane (0.1 ml/1 ml TRI reagent; Sigma, USA) was added. Following centrifugation, the resulting aqueous phase containing the RNA was transferred to a fresh column of GenElute Mammalian Total RNA Miniprep Kit (Sigma—Aldrich, USA) and RNA was isolated according to the manufacturer's protocol. The resulting RNA was reverse-transcribed to cDNA using Taq-Man reverse transcription reagents (Applied Biosystems, Foster City, USA). Finally, real-time polymerase chain reaction (PCR) was performed on a Quant Studio Flex 6 real-time PCR system (Applied Biosystems) under standard thermal conditions, using Taq-Man Universal PCR Master Mix (Applied Biosystems) and gene-specific primers and probes for aggrecan, collagen Type I and collagen Type II. These oligonucleotide primers and TaqMan probes (Table 1; all from Microsynth, Balgach, Switzerland) were designed using Primer Express Oligo Design software, versions 1.5/2.0 (Applied Biosystems). Probes were labelled with the reporter dye molecule FAM (6-carboxyfluorescein) at the 5′-end and with the quencher dye TAMRA (6-carboxy-N,N,N′,N′-tetramethylrhodamine) at the 3′-end. To exclude amplification of genomic DNA, the probe or one of the primers were selected to overlap an exon—exon junction. For PCR analysis, 18S ribosomal RNA TaqMan Gene Expression Assays (Applied Biosystems) was used as housekeeping gene. Relative quantification of target mRNA was performed according to the ΔΔCt method. Samples collected at Day 0 were used as reference for each group.

Table 1 Sequences of primers and probes used for RT-PCR.

Gene	Forward primer 5′-3′	Reverse primer 5′-3′	Probe 5′-3′
Aggrecan	CCA ACG AAA CCT ATG ACG TGT ACT	GCA CTC GTT GGC TGC CTC	ATG TTG CAT AGA AGA CCT CGC CCT CCA
Collagen I	TGC AGT AAC TTC GTG CCT AGC A	CGC GTG GTC CTC TAT CTC CA	CAT GCC AAT CCT TAC AAG AGG CAA CTG C
Collagen II	AAG AAA CAC ATC TGG TTT GGA GAA A	TGG GAG CCA GGT TGT CAT C	CAA CGG TGG CTT CCA CTT CAG CTA TGG

RT-PCR = real-time polymerase chain reaction.

Histological evaluation

Samples from each group were fixed for 30 min in 4% neutral buffered formalin at room temperature, embedded in cryosection medium and cut into 12-μm-thick sections. Toluidine blue, safranin O and fast green staining were performed, and sections were imaged in transmitted light using a BX63 (Olympus) microscope with a 20x objective.

Mechanical testing

Compression test was performed to evaluate the mechanical properties of the 3D-printed PCL scaffolds without and with microspheres. Cell-free and cell-containing microspheres were used to load the scaffolds. All groups were cultured in chondrogenic media for 42 days. The samples were then placed in a mechanical testing machine (Instron 5866, Norwood, MA, USA) with a load cell of 1000 N. The maximum load before damage (Nmax) in unconfined compression was determined on the pristine PCL 3D-printed construct. All samples were loaded at a displacement speed of 5 mm/min until reaching 30% of Nmax. The compressive modulus was obtained from the slope of the tangent of the strain–stress curves ($n = 3$) at 3 MPa.

Statistical analysis

Data are expressed as means ± standard deviation. Statistical differences between the groups were determined using unpaired two-tailed nonparametric Student's t-test with GraphPad Prism (version 7.00; GraphPad Software Inc., USA). Differences were considered statistically significant according to values of $^{*}P < 0.05$ and $^{**}P < 0.01$.

Results

Optimization of Alg-Gel electrospray microsphere fabrication

1.5% w: v alginate microspheres were initially produced by electrospray using the following experimental conditions: 10 kV/1 bar, 30 G, in 100 mM $CaCl_2$ as extensively reported elsewhere [10]. As expected, alginate microspheres were obtained (Figure 1A). In a second step, gelatin Type A at concentration of 1.0% and 2.5% w: v was added in 1:1 v:v ratio to the 1.5% w: v alginate. Coalescence of sprayed droplets was observed in all tested electrosprayed conditions, potentially due to the gelatin Type A low viscosity (data not shown). Hence, gelatin Type B was used instead, at three concentrations of 2.5, 1.5 and 0.5% w: v in the electrospray conditions previously tested (Figure 1B–D). The rounded morphology of the alginate microspheres was conserved in the 1.5% w: v alginate-0.5% w: v gelatin Type B group, while higher gelatin Type B concentrations led to ripple marks and loss of circularity.

The influence of the $CaCl_2$ coagulating bath concentration, 1% and 3% w: v $CaCl_2$, was assessed. 3% w: v $CaCl_2$ solution resulted in significantly more spherical microspheres than the 1% w: v $CaCl_2$ solution (Figure 2). Therefore, a 3% w: v $CaCl_2$ coagulating bath was chosen for the further optimization.

Then, the influence of voltage/air pressure and of the needle emitter size (inner diameters of 0.203 mm and 0.150 mm) were investigated; the circularity and diameter distribution of Alg-Gel Type B microspheres were calculated (Figure 3). The different combinations of voltage and air pressure as well as the selected needle emitters had no

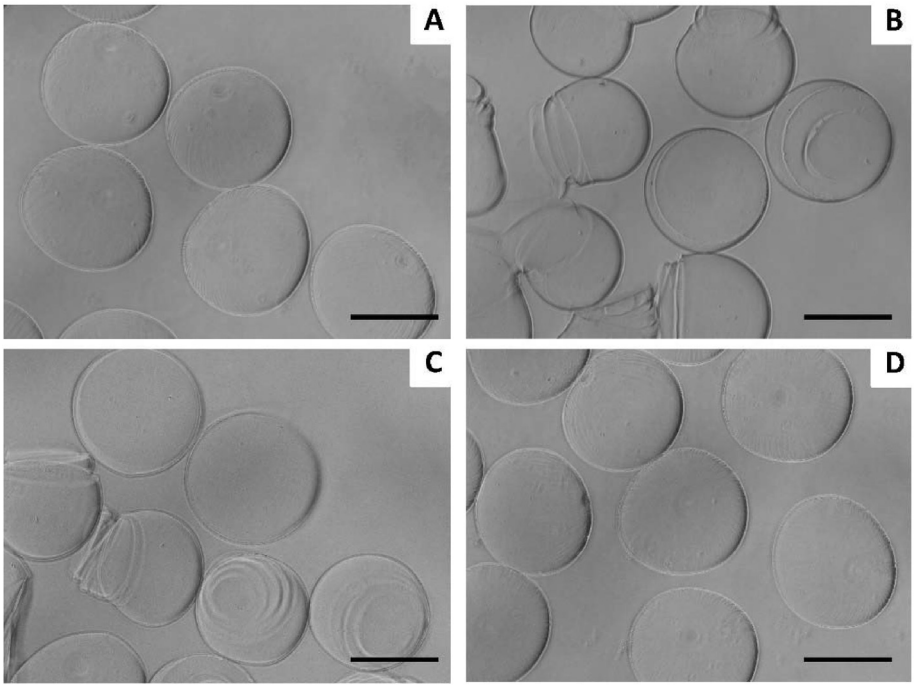

Figure 1 Representative microscopy image of (A) 1.5% w: v alginate microspheres, (B, C and D, respectively) 1.5% w: v alginate-2.5%, 1.5% and 0.5% w: v gelatin Type B produced by electrospray. Scale bar = 200 μm.

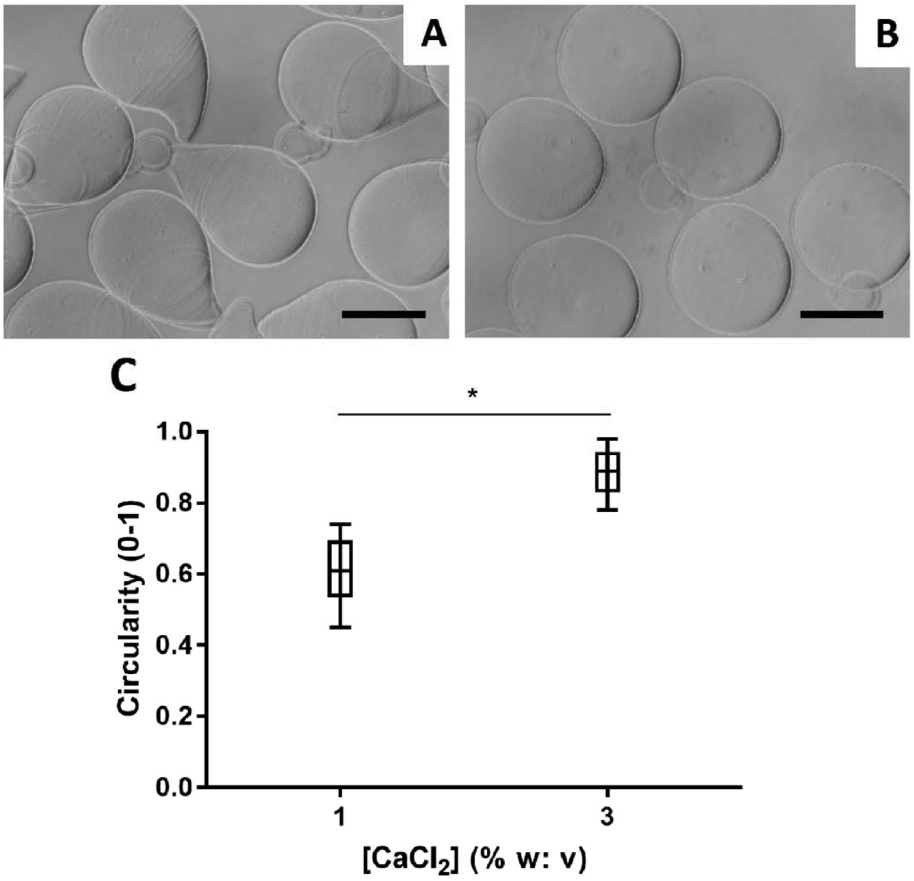

Figure 2 Representative microscopy image of 1.5% w: v alginate +0.5% w: v gelatin Type B produced by electrospray in (A) 1 and (B) 3% w: v $CaCl_2$ solution and (C) plot of the microspheres circularity as a function of the [$CaCl_2$] coagulating bath solution. Scale bar = 200 μm *P < 0.05.

significant effect on the circularity of microspheres under the chosen experimental conditions (Figure 3A and C, P>0.05). The average microsphere's diameters were respectively 240, 260 and 300 μm for 8/0.6, 8/1.0 and 6/1.0 kV/bar with a 0.150 mm needle emitter with a trend to larger microsphere size with decrease of air pressure and increase of voltage (Figure 3B). Increasing the needle emitter size from 0.150 mm (30 G) to 0.203 mm (27 G) led to an increase in the average microsphere diameter from 250 μm to 310 μm (Figure 3D). Overall, increasing the voltage and decreasing the flow rate lead to a decreased microspheres size. Besides, the increase of air pressure and decrease of voltage would produce a wider size distribution (Figure 3B).

Therefore, the following electrospray conditions were chosen for the hBMSCs embedding in Alg-Gel Type B microspheres:8 kV/0.6 bar and needle emitter of 0.150 mm inner diameter, with 3% w: v $CaCl_2$ coagulating bath.

hBMSCs embedding in Alg-Gel Type B electrospray microspheres

10×10^6 cells/ml hBMSCs were suspended in Alg-Gel, and microspheres were formed using the optimized experimental conditions. Representative microscopy images show similar morphology for the Alg-Gel with or without hBMSCs (Figure 4A and B). Circularity, average diameter (~250 μm) and size distributions were not significantly affected by the presence of hBMSCs at the concentration used (Figure 4C and D).

To confirm that the hBMSCs within the Alg-Gel microspheres generated by electrospray retain their viability after the manufacturing process, cell viability was assessed by live/dead and CellTiter-Blue assays. hBMSC metabolic activity assessed via CellTiter-Blue after electrospraying was above 95% of the control group (hBMSCs embedded in Alg-Gel gel) with no significant difference between these two groups (Figure 5C, P>0.05). A similar trend was observed by live/dead staining (Figure 6).

Assembly and maturation of hBMSCs in a 3D-printed PCL scaffold: a pilot study

Following the optimization of the electrospray fabrication method for hBMSCs embedded in Alg-Gel microspheres with high circularity, narrow polydispersity and average diameter of 250 μm, the Alg-Gel-hBMSCs microspheres were loaded into a 3D-printed PCL scaffold and cultured for 14 days in proliferation media in well plates. Additional groups consisted in Alg-hBMSCs and Alg-Gel-hBMSCs in 2D well plate culture, and Alg-Gel-hBMSCs in 3D bioreactor culture.

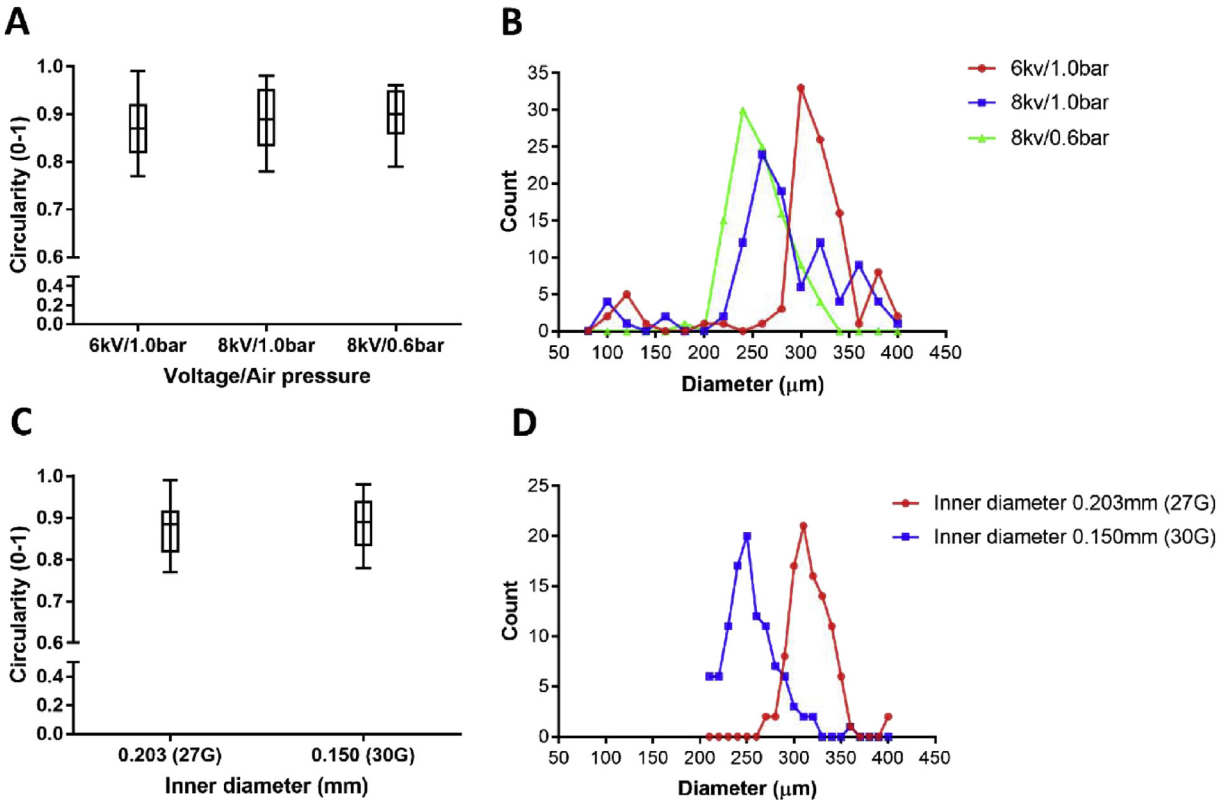

Figure 3 (A) Plot of the microspheres circularity as a function of the voltage and air pressure; (B) influence of the voltage and air pressure on microsphere diameters distribution; (C) plot of the microspheres circularity as a function of the needle size; (D) influence of the needle size on microsphere diameters distribution. 100 microspheres were measured in each group.

The inner porosity of the 3D-printed PCL was designed in this study as a 200 μm interspace for the bottom layer and 800 μm for the middle layers. This special design ensured that the seeded electrospray microspheres would get enough space to grow and connect into larger tissues but could not leak out from the bottom layer during the initial culture period. The porosity was optimized for ease of microspheres loading with a diameter between 200 μm and 250 μm. Owing to the thickness of the printed bioink line, the line space was finally measured as 0.7 mm at the bottom layer and 1.5 mm at the middle layers by BioCAD. For 1 ml Alg-Gel hydrogel solution, around 9000 microspheres were collected after electrospraying; therefore, according to this yield, the diameter and height of PCL scaffold was decided as 12 mm and 5 mm (10 layers in total), respectively. Lastly, all the microspheres from each sample were moved into the 3D structure using a 2-ml syringe with a 25-G needle.

At Day 0, all groups have a high and similar hBMSC viability (Figure 6). For the Alg-hBMSCs+2D group, dead cells (red) were observed from Day 3 and their number increased up to Day 14. Comparing to Alg-hBMSCs, cell death within the microspheres containing gelatin was less pronounced up to 14 days, indicating the beneficial effect of the gelatin on the preservation of hBMSC viability in alginate microspheres. The Alg-Gel-hBMSCs cultured in 3D-printed PCL scaffold in 2D well plate and the Alg-Gel-hBMSCs cultured in 3D bioreactor had a similar cell viability, higher than the two previous groups, and both showed significantly higher cell number per microspheres at 14 days compared to Day 0.

hBMSC proliferation was assessed by CellTiter-Blue (Figure 7A). Proliferation of hBMSCs embedded in gelatin-containing electrosprayed alginate microspheres was significantly higher in comparison to alginate microspheres. Culture in a rotating 3D bioreactor enhanced further the proliferation of hBMSCs embedded in Alg-Gel microspheres in comparison to all other groups. Interestingly, the proliferation of hBMSCs embedded in Alg-Gel microspheres seeded in PCL 3D-printed scaffolds (Alg-Gel-hBMSCs+PCL+2D group) showed a proliferation curve that was intermediate between the static 2D and the 3D bioreactor culture.

Following this initial study, a longer term culture of 42 days was set and three groups (Alg-Gel-hBMSCs+2D, Alg-Gel-hBMSCs+PCL+2D and Alg-Gel-hBMSCs+3D) were cultured in chondrogenic medium. The DNA content of all three groups significantly increased during culture time ($P < 0.05$). At all time points, the DNA content of the Alg-Gel-hBMSCs+3D group was higher than that of the Alg-Gel-hBMSCs+PCL+2D group ($P < 0.05$), and the DNA content of the Alg-Gel-hBMSCs+PCL+2D group was higher than that of the Alg-Gel-hBMSCs+2D group ($P < 0.05$, Figure 7B). Similarly, the GAG content of all three groups significantly increased during the culture period ($P < 0.05$), and the GAG content of the Alg-Gel-hBMSCs+3D group was higher than that of the Alg-Gel-hBMSCs+PCL+2D group ($P < 0.05$) until Day 21 with no significant difference at Day 42 (P˃0.05). The

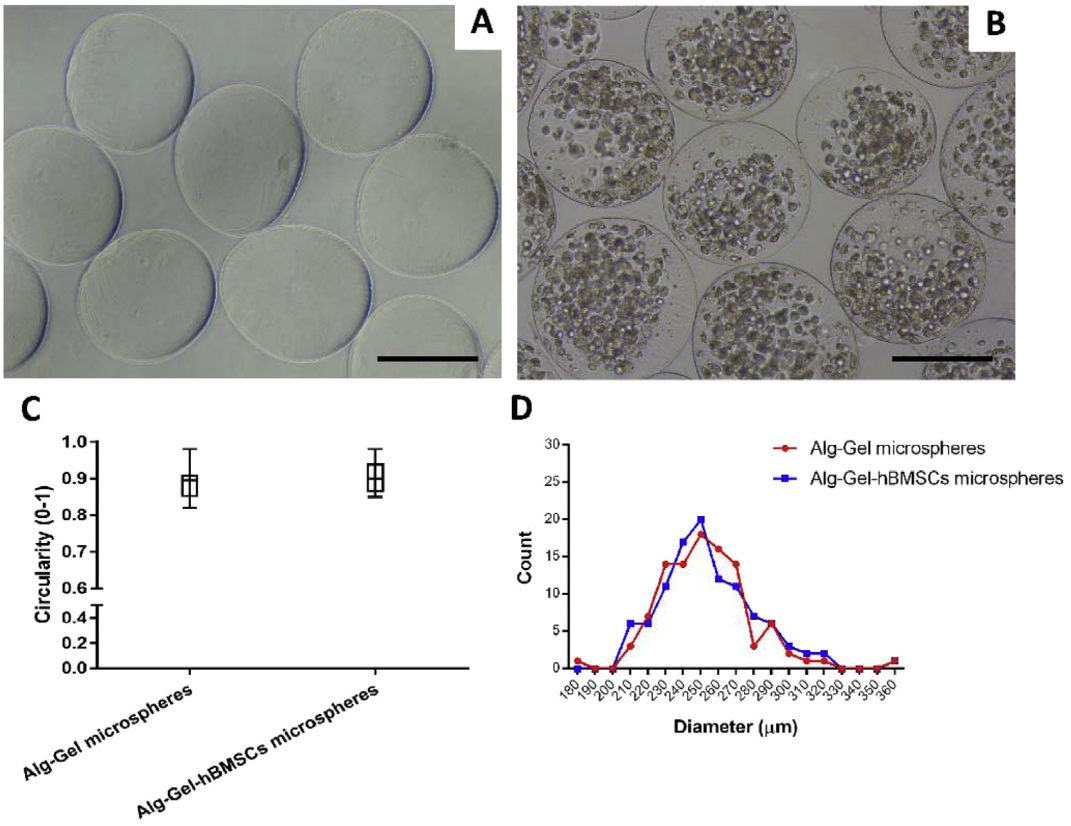

Figure 4 Representative microscopy images of optimized Alg-Gel microspheres (A) without hBMSCs and (B) containing 10×10^6 hBMSCs in 1 ml Alg-Gel produced using the optimized electrospray protocol; (C) plot of the microspheres circularity with or without hBMSCs; (D) influence of the hBMSCs on microsphere diameters distribution. Scale bar = 200 μm. 100 microspheres were measured in each group. hBMSCs = human bone marrow stromal cells.

GAG content in the Alg-Gel-hBMSCs+PCL+2D group was higher than that of the Alg-Gel-hBMSCs+2D group after 14 days ($P < 0.05$, Figure 7C). The GAG/DNA ratio increased in all three groups from Day 0 to Day 7 ($P < 0.05$). The GAG/DNA value of the Alg-Gel-hBMSCs+PCL+2D group increased significantly until Day 21 ($P < 0.05$). On Day 21 and 42, GAG/DNA ratio of the Alg-Gel-hBMSCs+PCL+2D group was higher than that of the Alg-Gel-hBMSCs+2D group ($P < 0.05$). There was no significant difference in the GAG/DNA values of the Alg-Gel-hBMSCs+PCL+2D group and the Alg-Gel-hBMSCs+3D group ($P > 0.05$, Figure 7D).

At Day 21 and 42, all the three tested groups had higher expression of the characteristic chondrogenic genes, namely aggrecan and collagen Type II, in comparison to the hBMSCs in Alg-Gel microspheres produced by electrospray at Day 0 (Figure 8). Aggrecan expression was significantly higher in the Alg-Gel-hBMSCs+3D group than in the other two groups on Day 21 ($P < 0.05$), and aggrecan expression in the Alg-Gel-hBMSCs+PCL+2D group was significantly higher than that in the Alg-Gel-hBMSCs+2D group on Day 42 ($P < 0.05$). The Alg-Gel-hBMSCs+3D group had no significant difference with Alg-Gel-hBMSCs+PCL+2D group on Day 42 ($P > 0.05$, Figure 8A). For collagen Type I, the Alg-Gel-hBMSCs+2D group was significantly higher than the Alg-Gel-hBMSCs+3D group ($P < 0.05$), which was also higher than the Alg-Gel-hBMSCs+PCL+2D group on Day 21 ($P < 0.05$). On Day 42, the Alg-Gel-hBMSCs+2D group was significantly higher than the other two groups ($P < 0.05$), and there was no significant difference between Alg-Gel-hBMSCs+PCL+2D and Alg-Gel-hBMSCs+3D groups ($P > 0.05$, Figure 8B). For collagen Type II, similar to the trends observed for aggrecan, the Alg-Gel-hBMSCs+3D group was significantly higher than the other two groups on Day 21 ($P < 0.05$). On Day 42, the Alg-Gel-hBMSCs+2D group was significantly lower than the other two groups ($P < 0.05$). There was no significant difference between Alg-Gel-hBMSCs+PCL+2D and Alg-Gel-hBMSCs+3D groups on Day 42 ($P > 0.05$, Figure 8C).

Histology sections were performed at 42 days, and two general matrix staining was performed (Figure 9). In all cases, alginate material gave a strong background signal. Nonetheless, matrix deposition, mainly pericellular, was qualitatively the highest in the Alg-Gel-hBMSCs+3D group, then Alg-Gel-hBMSCs+2D and finally, the Alg-Gel-hBMSCs+PCL+2D.

Stress—strain relation and slops were examined of all the 3 groups ($n = 3$) on Day 42. All the samples were loaded until 30% Nmax was reached, which corresponds to a nominal stress (σe) of 5.30 MPa. The samples had a final strain (εe) of $4.544 \pm 0.068\%$ in the PCL group and $5.023 \pm 0.206\%$ in the Alg-Gel+PCL group, and there is no significant difference between these two groups ($P > 0.05$). However, the final strain of the Alg-Gel-hBMSCs+PCL group was $10.73 \pm 0.44\%$, which was significant difference from the other two groups ($P < 0.05$). The slope of stress—strain in each group at 2.65 MPa, the half of final stress, reflected

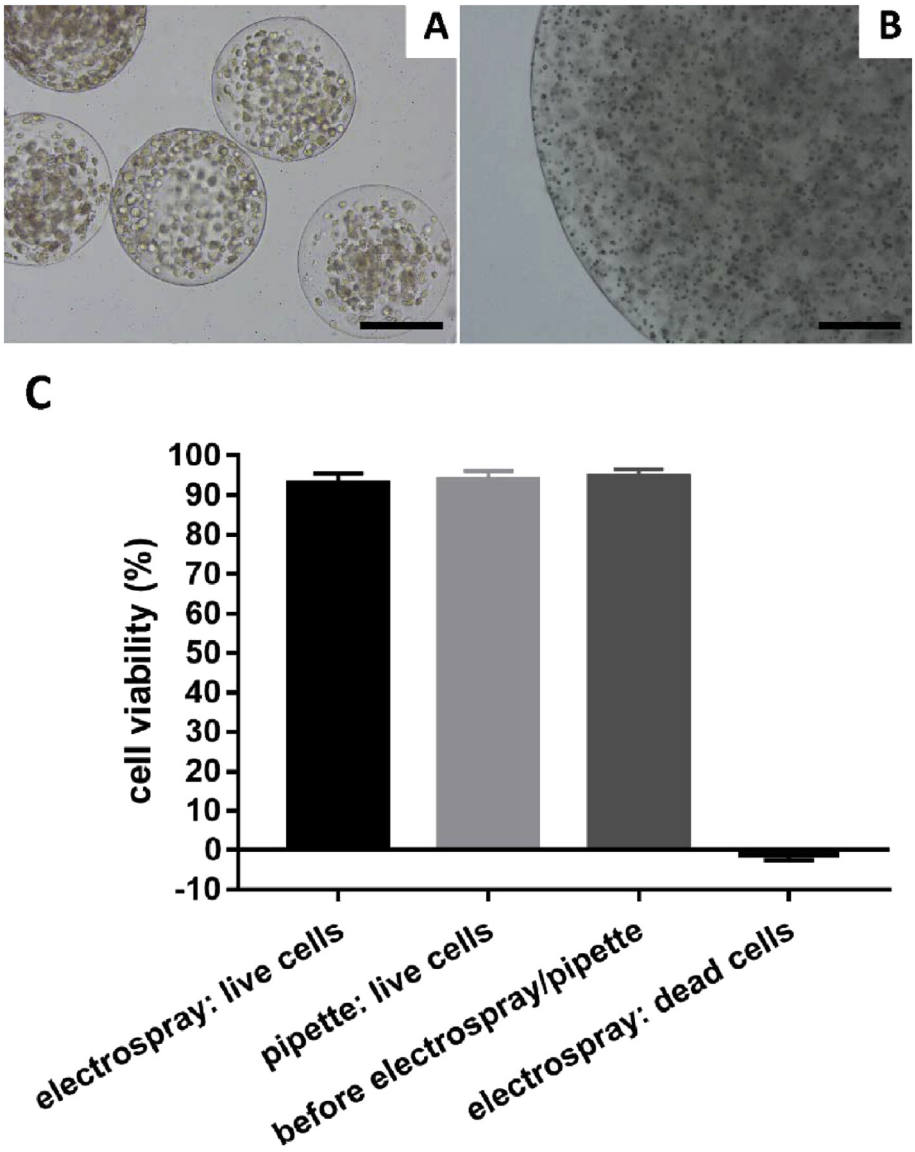

Figure 5 Representative image of hBMSCs (A) containing microspheres produced by electrospray and (B) containing macrogel produced using a pipette and dropping into coagulating bath; (C) plot of the hBMSC cell viability (metabolic activity relative to cell before electrospray/pipette) using the two methods of electrospray and pipetting. Scale bar = 200 μm. hBMSCs = human bone marrow stromal cells.

the trend change: 1.873 ± 0.067 MPa in the PCL group was not significantly different from 1.938 ± 0.099 MPa for the Alg-Gel+PCL group (P>0.05) and 0.860 ± 0.073 MPa for the Alg-Gel-hBMSCs+PCL group, which was lower than the other two groups ($P < 0.05$).

Discussion

In this study, the electrospray manufacturing of Alg-Gel hydrogel microspheres containing hBMSCs with high viability and proliferative capacity was optimized. Under different culture conditions in chondrogenic media, namely static, static seeded in 3D-printed scaffold and dynamic seeded in 3D-printed scaffold (3D bioreactor), DNA and GAG contents increased from the former to the latest. Real-time PCR analysis indicated that main chondrogenic genes (Type II collagen and aggrecan) were upregulated, while Type I collagen was upregulated to a less strong extent.

Microparticles and nanoparticles obtained by electrospray can show higher loading efficiency and narrow particle size distribution compared to particles obtained by other techniques [18]. Furthermore, the need for particle separation from dispersing solution or even removal of nondegradable surfactants used in some of the fabrication techniques are prevented, thus making it a technique of choice for cell embedding [18—21]. The different process parameters of the electrospray need to be optimized and controlled as they influence the size, circularity and polydispersity of the particles, and a suboptimal process results in a break of the jet into droplets giving rise to particles of different sizes and shapes [18,21,22].

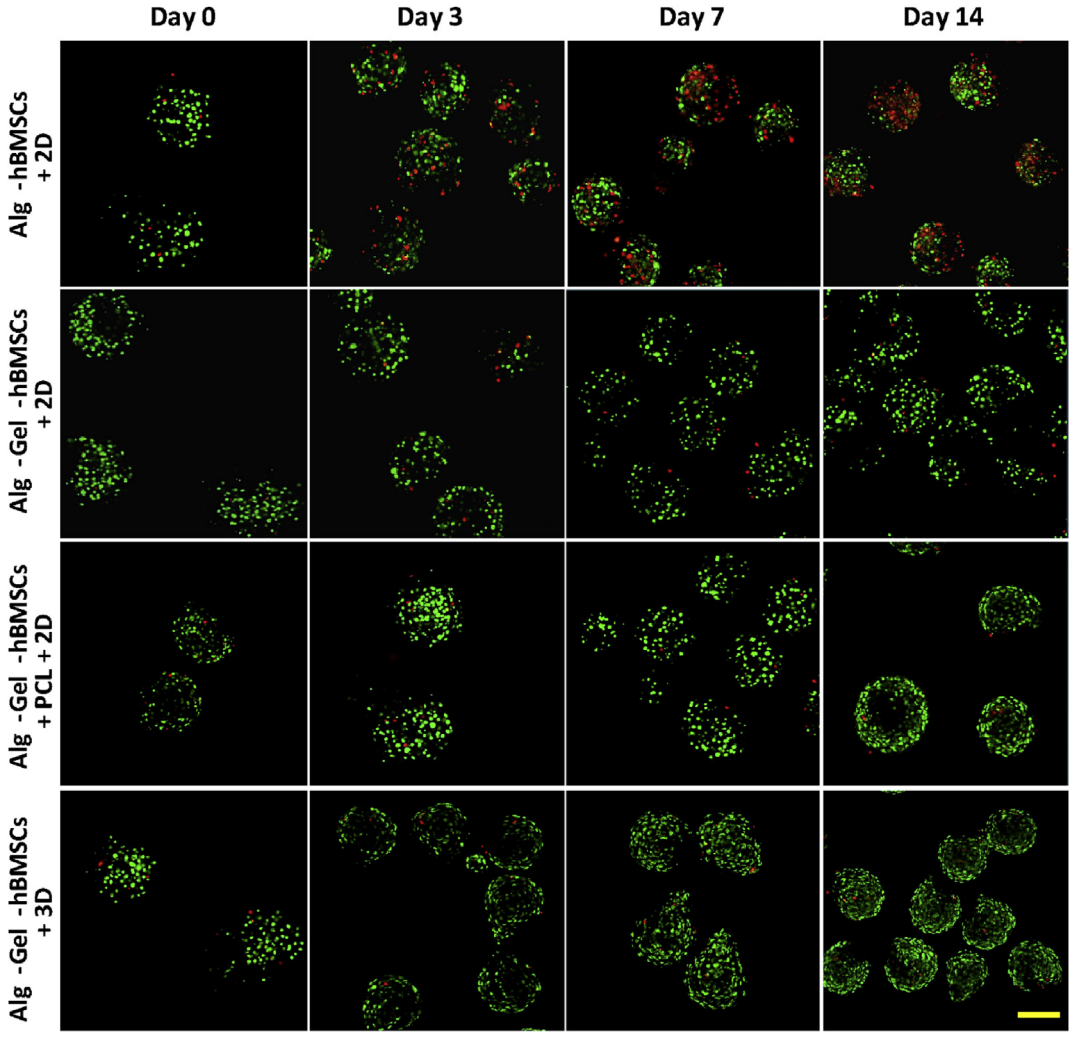

Figure 6 Live/Dead staining of Alg-hBMSCs with 2D well plate culture, Alg-Gel-hBMSCs with 2D well plate culture, Alg-Gel-hBMSCs + 3D-printed PCL scaffold with 2D well plate culture and Alg-Gel-hBMSCs with 3D bioreactor culture on Day 0, 3, 7 and 14, respectively. Scale bar = 200 μm. hBMSCs = human bone marrow stromal cells; PCL = poly(ε-caprolactone).

With gelatin Type A added, alginate microspheres could not be produced and aggregated macrogels were formed. This is likely due to coalescence of sprayed droplets related to the influence of the gelatin Type A on the viscosity of the Alg-Gel solution. With the same concentrations of gelatin Type B, Alg-Gel microspheres were successfully formed at various alginate concentrations. 0.5% w: v was found to be the optimal concentration for the production of spherical microspheres. An optimal combination of the electrospray parameters and properties of Alg-Gel hydrogel were established in this study following the single variable principle, which provided a guideline for the biofabrication of microspheres: 1.5% w: v alginate − 0.5% w: v gelatin (Type B) with a concentration of 10×10^6 hBMSCs/ml, produced by electrospray with the parameters of 30G needle size, 3% w: v $CaCl_2$ coagulating bath, and 8 kV voltage and 0.6 bar air pressure. Interestingly, adding 10×10^6 hBMSCs/ml, relevant for cartilage TE maturation, did not modify the microsphere morphology, allowing the conservation of the optimized parameters, which is seldom achieved with bioinks.

Another technique was used for providing a macrostructural environment or scaffold for microspheres assembly, namely fuse deposition modelling. Such technique allows complex 3D structures to be designed and developed in computer-aided design using the geometrical data obtained from medical imaging techniques such as X-ray imaging, microcomputerized tomography and magnetic resonance imaging [23—25]. Three-dimensional printing of tissue constructs allows exact placement of multiple cell types, biomaterials and scaffolds in predefined positions within the 3D structures. To date, direct printing of cells embedded in bioinks is still a difficult task when high cell content, viability and initial high mechanical stability are required. However, comparing to cell dispersion and even scaffold-based TE, the abilities to control cell distribution in the 3D structures and using multibiological components to deliver multiple cell types to specific locations are an obvious advantage of 3D bioprinting [26]. Therefore, a possible approach is to seed microtissue-like particles providing a suitable environment for cell differentiation and matrix formation in a 3D-printed scaffold providing the

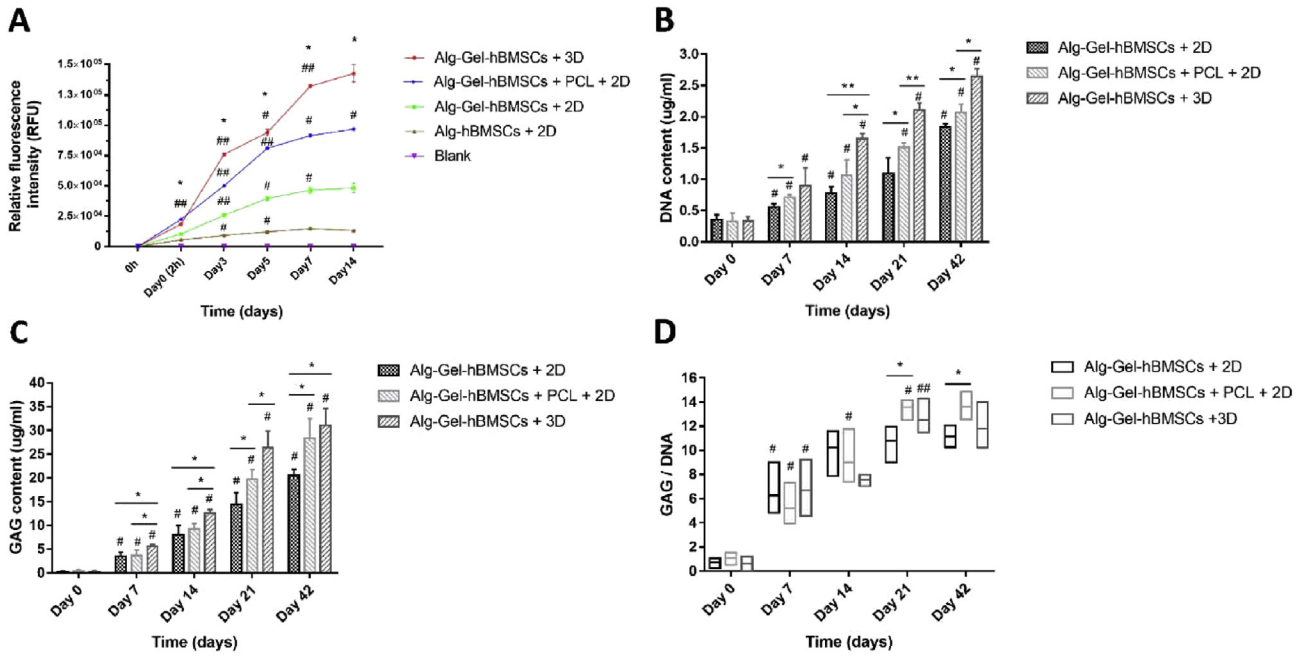

Figure 7 Plot of the CellTiter-Blue biochemical assay representing the proliferation of hBMSCs embedded in alginate- and gelatin-containing electrosprayed alginate microspheres cultured under different conditions improves (A) proliferation, (B) the DNA content, (C) GAG content and (D) GAG/DNA ratio of the Alg-Gel-hBMSCs with 2D culture group, Alg-Gel-hBMSCs + 3D-printed PCL scaffold with 2D culture group and Alg-Gel-hBMSCs with 3D bioreactor culture group over a culture period of 42 days. *$p < 0.05$, **$p < 0.01$, significant difference between groups; #$p < 0.05$, ##$p < 0.01$, significantly different from the previous time point. hBMSCs = human bone marrow stromal cells; PCL = poly(ε-caprolactone).

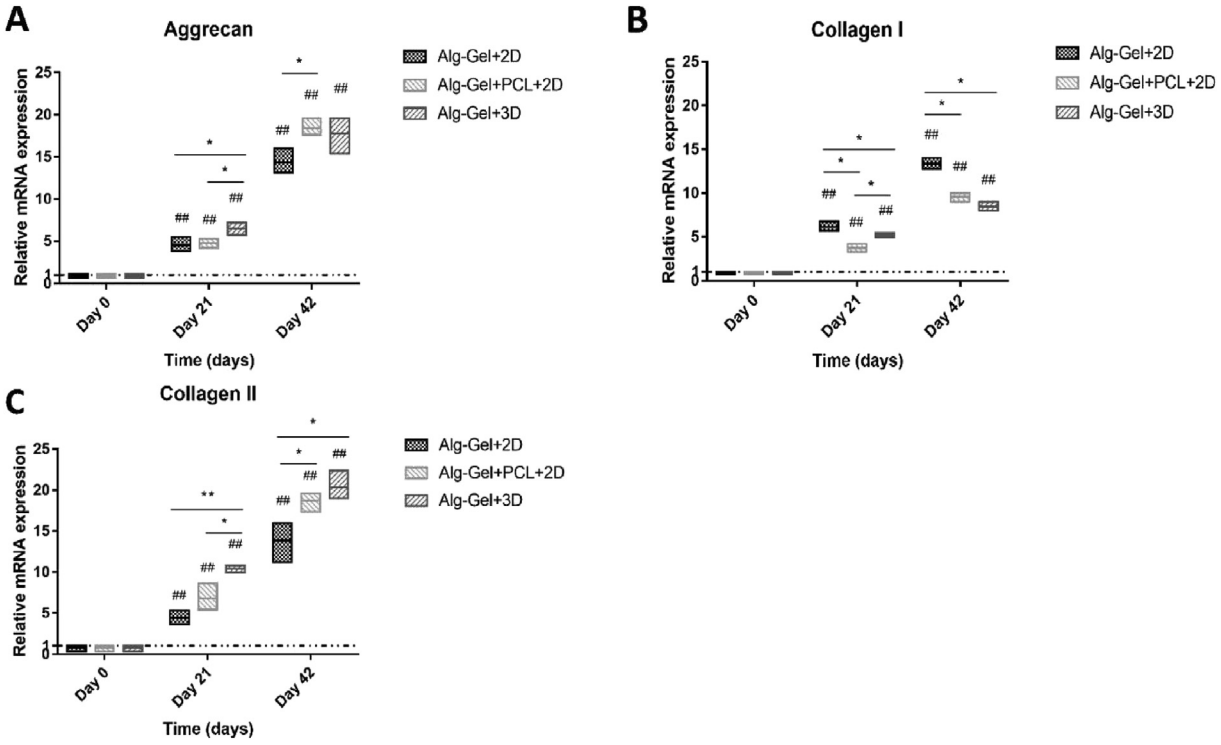

Figure 8 Chondrogenic differentiation markers ((A) aggrecan, (B) collagen Type I and (C) Type II) expression of Alg-Gel-hBMSCs with 2D culture group, Alg-Gel-hBMSCs + 3D-printed PCL scaffold with 2D culture group and Alg-Gel-hBMSCs with 3D bioreactor culture group on Day 21 and 42 respectively. *$p < 0.05$, **$p < 0.01$, significant difference between groups; #$p < 0.05$, ##$p < 0.01$, significantly different from Day 0 (reference). hBMSCs = human bone marrow stromal cells; PCL = poly(ε-caprolactone).

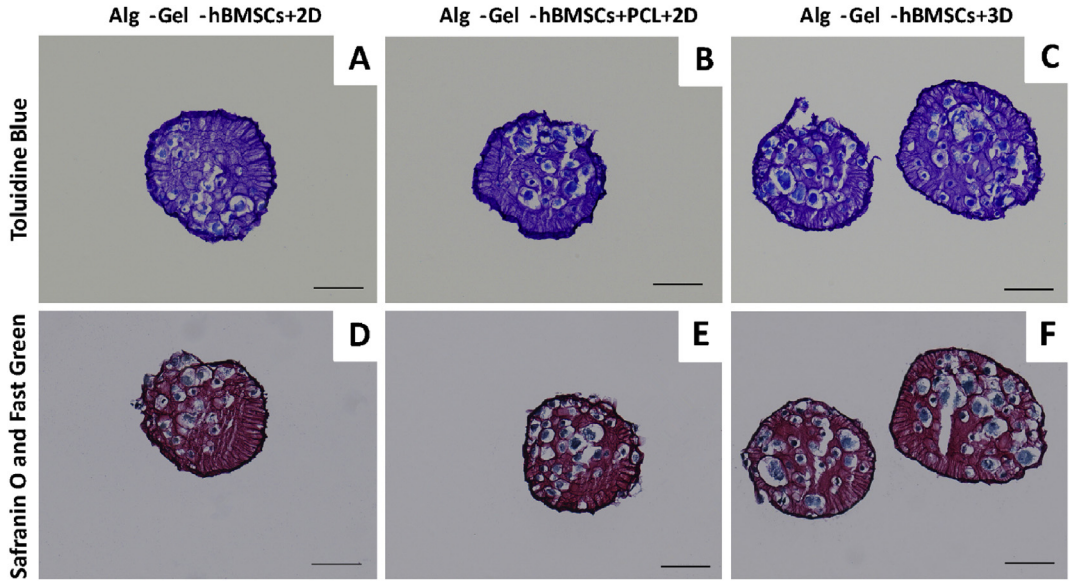

Figure 9 Representative images of (A—C) toluidine blue and (D—F) safranin O & fast green stained histology sections of the Alg-Gel-hBMSCs with 2D well plate culture, Alg-Gel-hBMSCs + 3D-printed PCL scaffold with 2D well plate culture and Alg-Gel-hBMSCs with 3D bioreactor culture on Day 42. Scale bar = 100 μm. hBMSCs = human bone marrow stromal cells; PCL = poly(ε-caprolactone).

initial mechanical stability required for tissue-engineered constructs implanted in load-bearing tissue such as articular cartilage [27,28].

For the successful isolation and expansion of stem cells from a variety of sources, appropriate culture protocols (e.g. mimicking their specialized microenvironment) are essential. Alginate and gelatin are the biomaterials that offer great potential in TE applications, including biocompatibility, low toxicity, relatively low cost and mild gelation [29]. Alg-Gel hydrogels provide 3D extracellular matrices for living tissues allowing delivery of bioactive compounds and provide attachment sites to cells. Several studies have been carried out on Alg-Gel as scaffold and ECM alternative for differentiation of BMSCs into chondrogenic purposes [29,30]. Importantly, it has been shown that 3D hydrogel culture of MSCs was superior to pellet culture in preventing terminal differentiation and hypertrophy [31]. In addition, the RCCS, a 3D dynamic culture system, facilitates more efficient gas, liquid, oxygen, nutrient and waste transfer [32]. The RCCS also provides a simulated microgravity environment to effectively induce chondrogenesis [33]. The results demonstrated that aggrecan and collagen Type II gene expression levels were significantly higher in the 3D bioreactor group and 3D-printed PCL scaffold group compared to cells in the 2D well plate group. We hypothesized that this could be the results of improved nutrient exchange in 3D versus 2D and possibly cell outgrowth on PCL 3D scaffolds leading to a higher surface area available for cell proliferation. Interestingly, this does not influence negatively the differentiation. Conversely, microgravity and 3D environment markedly enhanced the chondrogenesis. These were consistent with the previous observations of Ohyabu and Bo, who reported that the continuous mechanical stress caused by medium flow and microgravity associated with low shear facilitate the chondrogenesis of stem cell [33,34], and Yin et al. [35], who indicated that BMSCs cultured in RCCS showed both better proliferation and better chondrogenic differentiation compared with the 2D cell controls. However, it has been shown that hMSCs embedded in alginate beads have an increase of collagen Type X gene expression, sign of hypertrophy at 2 and 4 weeks when cultured in static conditions [36]. Thus, an increase of collagen Type X expression cannot be ruled in our different groups used. This could be addressed in a following study via improved cell culture conditions for example [37].

As mentioned previously, the 3D bioreactor group and 3D-printed PCL scaffold group had a higher level of both cell proliferation and chondrogenic differentiation, as reflected by Live/Dead staining, quantification of CellTiter-Blue, DNA content, GAG content and GAG/DNA ratio. As Figuer 7B and C showed, the DNA content and GAG content were increasing over time, especially in the 3D bioreactor group and 3D-printed PCL scaffold group. Matrix accumulation in the microspheres was also confirmed by histology. On the other gene level, the aggrecan and collagen Type I and Type II gene expression also provided a useful insight about the chondrogenic differentiation. For aggrecan and collagen Type II, the gene expression was increasing with time and was significantly higher in the 3D bioreactor group and 3D-printed PCL scaffold group compared to the 2D control. For collagen Type I, it is expected that the level of expression would continually increase during in vitro culture for all groups, but as Figure 8B showed, the collagen Type I expression in the 2D well plate group was higher than in the other two groups, which indicated that the chondrogenic differentiation in the first group was not as good as the other two groups.

No significant difference in the strain—stress curves of 3D-printed PCL scaffold, with or without Alg-Gel

microspheres inside, was observed. The overall mechanical property of the TE construct is given by the PCL 3D-printed structure and conserved during the 42 days of culture. PCL is a slow biodegradable polyester, and complete clearance of the polymer in vivo may take up to 2—4 years [38]. PCL scaffolds seeded with chondrocyte in an osteochondral rabbit model for 3 months did not degrade [39]. Use of faster degradable biocompatible thermoplastic polymers may be beneficially to replace PCL, even though long-term studies (>1—2 years) of the behaviour of PCL-based TE constructs implanted in articular cartilage are not yet available and no detrimental effect on the repair tissue quality was reported [39]. Interestingly, in the hBMSC-containing group, the initial profile is different, with a reduced slope, which suggests matrix production and deposition on the surface of the 3D-printed microsphere-containing scaffolds. Thus, matrix deposition occurs not only in the interspace of the scaffold within the microspheres, but also on the top and surfaces of the PCL. Further work is required to verify and complete the proof of concept presented in this study, such as the replication of the study with several hBMSCs donors and additional proof of the chondrogenic differentiation and prevention of hypertrophy; however, the use of calibrated hBMSC electrospray microspheres and their facile assembly in designed 3D-printed structure for fabrication of cartilage TE was demonstrated.

Conclusions

Alg-Gel microspheres produced by electrospray had an excellent cytocompatibility and promoted the stem cell proliferation. The Alg-Gel composition selected maintained a higher level of hBMSC viability in comparison to alginate microspheres and supported chondrogenesis in vitro. Seeding and assembly of microspheres in 3D-printed PCL scaffolds and culture in a 3D bioreactor were achieved, and biochemical assays as well as gene expression results indicated that hBMSCs could be differentiated toward a chondrogenic phenotype.

Conflicts of Interest

All the authors have no conflict of interest to disclose.

Acknowledgements

This study was funded by the Sino Swiss Science and Technology Cooperation [SSSTC, No. EG08-122016]. Dr. Yichi Xu is grateful for the support from the China Scholarship Council [CSC, No. 201703170097].

References

[1] Vinatier C, Guicheux J. Cartilage tissue engineering: from biomaterials and stem cells to osteoarthritis treatments. Ann Phys Rehabil Med 2016;59(3):139—44.
[2] Haleem AM, Chu CR. Advances in tissue engineering techniques for articular cartilage repair. Operat Tech Orthop 2010; 20(2):76—89.
[3] Langer R, Vacanti JP. Tissue engineering. Science 1993; 260(5110):920—6.
[4] Ikada Y. Challenges in tissue engineering. J R Soc Interface 2006;3(10):589—601.
[5] Vinatier Claire. Cartilage tissue engineering: towards a biomaterial-assisted mesenchymal stem cell therapy. Curr Stem Cell Res Ther 2009;4(4):318—29.
[6] Ahmed EM. Hydrogel: preparation, characterization, and applications: a review. J Adv Res 2015;6(2):105—21.
[7] Hunt JA, Rui C, Veen TV, Bryan N. Hydrogels for tissue engineering and regenerative medicine. J Mater Chem B 2014; 2(33):5319—38.
[8] Wang L, Shelton RM, Cooper PR, Lawson M, Triffitt JT, Barralet JE. Evaluation of sodium alginate for bone marrow cell tissue engineering. Biomaterials 2003;24(20):3475—81.
[9] Deepthi S, Jayakumar R. Alginate nanobeads interspersed fibrin network as in situ forming hydrogel for soft tissue engineering. Bioact Mater 2018;3(2):194—200.
[10] Yao R, Zhang R, Luan J, Lin F. Alginate and alginate/gelatin microspheres for human adipose-derived stem cell encapsulation and differentiation. Biofabrication 2012;4(2): 25007—10.
[11] Song K, Li L, Li R, Lim M, Liu P, Liu T. Preparation, mass diffusion, and biocompatibility analysis of porous-channel controlled calcium-alginate-gelatin hybrid microbeads for in vitro culture of NSCs. Appl Biochem Biotechnol 2014;173(3): 838—50.
[12] Lee KY, Mooney DJ. Hydrogels for tissue engineering. Chem Rev 2001;101(7):1869—79.
[13] Xu M, Wang X, Yan Y, Yao R, Ge Y. An cell-assembly derived physiological 3D model of the metabolic syndrome, based on adipose-derived stromal cells and a gelatin/alginate/fibrinogen matrix. Biomaterials 2010;31(14):3868—77.
[14] Matricardi P, Di MC, Coviello T, Hennink WE, Alhaique F. Interpenetrating Polymer Networks polysaccharide hydrogels for drug delivery and tissue engineering. Adv Drug Deliv Rev 2013;65(9):1172—87.
[15] Lennon DP, Caplan AI. Isolation of human marrow-derived mesenchymal stem cells. Exp Hematol 2006;34(11):1604—5.
[16] Gantenbein-Ritter B, Sprecher CM, Chan S, Illien-Jünger S, Grad S. Confocal imaging protocols for live/dead staining in three-dimensional carriers. Method Mol Biol 2011;740:127.
[17] Reno C, Marchuk L, Sciore P, Frank CB, Hart DA. Rapid isolation of total RNA from small samples of hypocellular, dense connective tissues. Biotechniques 1997;22(6):1082—6.
[18] Zamani M, Prabhakaran MP, Ramakrishna S. Advances in drug delivery via electrospun and electrosprayed nanomaterials. Int J Nanomed 2013;8:2997—3017.
[19] Hao S, Wang Y, Wang B, Deng J, Zhu L, Cao Y. Formulation of porous poly(lactic-co-glycolic acid) microparticles by electrospray deposition method for controlled drug release. Mater Sci Eng C 2014;39:113—9.
[20] Jayaraman P, Gandhimathi C, Venugopal JR, Becker DL, Ramakrishna S, Srinivasan DK. Controlled release of drugs in electrosprayed nanoparticles for bone tissue engineering. Adv Drug Deliv Rev 2015;94:77—95.
[21] Ma Z, Ji H, Teng Y, Dong G, Zhou J, Tan D, et al. Engineering and optimization of nano- and mesoporous silica fibers using sol—gel and electrospinning techniques for sorption of heavy metal ions. J Coll Inter Sci 2011;358(2):547—53.
[22] Nazari M, Muddiman DC. Cellular-level mass spectrometry imaging using infrared matrix-assisted laser desorption electrospray ionization (IR-MALDESI) by oversampling. Anal Bioanal Chem 2015;407(8):2265—71.
[23] Guillotin B, Souquet AS, Duocastella M, Pippenger B, Bellance S, Bareille R, et al. Laser assisted bioprinting of engineered tissue with high cell density and microscale organization. Biomaterials 2010;31(28):7250—6.

[24] Guvendiren M, Molde J, Soares RM, Kohn J. Designing biomaterials for 3D printing. ACS Biomater Sci Eng 2016;2(10):1679—93.
[25] Xu Y, Meng H, Yin H, Sun Z, Peng J, Xu X, et al. Quantifying the degradation of degradable implants and bone formation in the femoral condyle using micro-CT 3D reconstruction. Exp Ther Med 2018;15(1):93—102.
[26] Park JY, Gao G, Jang J, Cho DW. 3D printed structures for delivery of biomolecules and cells: tissue repair and regeneration. J Mater Chem B 2016;4(47):7521—39.
[27] Murphy SV, Atala A. 3D bioprinting of tissues and organs. Nat Biotechnol 2014;32(8):773—85.
[28] Lee H, Cho DW. One-step fabrication of an organ-on-a-chip with spatial heterogeneity using a 3D bioprinting technology. Lab Chip 2016;16(14):2618—25.
[29] Venkatesan J, Bhatnagar I, Manivasagan P, Kang KH, Kim SK. Alginate composites for bone tissue engineering: a review. Int J Biol Macromol 2015;72:269—81.
[30] Wong M. Alginates in tissue engineering. Methods Mol Biol 2004;238:77—86.
[31] Watts AE, Ackerman-Yost JC, Nixon AJ. A comparison of three-dimensional culture systems to evaluate in vitro chondrogenesis of equine bone marrow-derived mesenchymal stem cells. Tissue Eng A 2013;19(19—20):2275—83.
[32] Cummings LJ, Waters SL. Tissue growth in a rotating bioreactor. Part II: fluid flow and nutrient transport problems. Math Med Biol 2007;24(2):169—208.
[33] Gao H, Ayyaswamy PS, Ducheyne P. Dynamics of a microcarrier particle in the simulated microgravity environment of a rotating-wall vessel. Microgravity Sci Technol 1997;10(3):154—65.
[34] Ohyabu Y, Kida N, Kojima H, Taguchi T, Tanaka J, Uemura T. Cartilaginous tissue formation from bone marrow cells using rotating wall vessel (RWV) bioreactor. Biotechnol Bioeng 2010;95(5):1003—8.
[35] Yin H, Wang Y, Sun Z, Sun X, Xu Y, Li P, et al. Induction of mesenchymal stem cell chondrogenic differentiation and functional cartilage microtissue formation for in vivo cartilage regeneration by cartilage extracellular matrix-derived particles. Acta Biomater 2016;33:96—109.
[36] Ma HL, Hung SC, Lin SY, Chen YL, Lo WH. Chondrogenesis of human mesenchymal stem cells encapsulated in alginate beads. J Biomed Mater Res A 2010;64A(2).
[37] Bian L, Zhai DY, Zhang EC, Mauck RL, Burdick JA. Dynamic compressive loading enhances cartilage matrix synthesis and distribution and suppresses hypertrophy in hMSC-laden hyaluronic acid hydrogels. Tissue Eng A 2012;18(7—8):715—24.
[38] Woodruff MA, Hutmacher D. The return of a forgotten polymer—polycaprolactone in the 21st century. Prog Polym Sci 2010;35(10):1217—56.
[39] Martinez-Diaz S, Garcia-Giralt N, Lebourg M, Gómez-Tejedor JA, Vila G, Caceres E, et al. In vivo evaluation of 3-dimensional polycaprolactone scaffolds for cartilage repair in rabbits. Am J Sports Med 2010;38(3):509.